IARJSET

ISSN (O) 2393-8021, ISSN (P) 2394-1588

International Advanced Research Journal in Science, Engineering and Technology

Impact Factor 8.066 ⁜ Peer-reviewed & Refereed journal ⁜ Vol. 12, Issue 4, April 2025

DOI: 10.17148/IARJSET.2025.124104

Numerical Investigation of Propeller–Wing Integration and Its Effect on Aerodynamic Characteristics at Various Rotational Speeds

G. Shiva Krishna,M.E.[1], D.V.Sai Mohit[2], K. Vinnisha[3], Dilleswara Rao Peddi,M.E.[4]

Assistant Professor, Aeronautical Department, Institute Of Aeronautical Engineering, Hyderabad, India[1]

UG student, Aeronautical Department, Institute Of Aeronautical Engineering, Hyderabad, India[2,3]

Project Associate, CTFD Department, CSIR-NAL, Bangalore, India[4]

Abstract: Propeller–wing aerodynamic interaction is critical in aircraft performance, especially in configurations involving closely integrated components. This study presents a CFD-based analysis of a scaled three-bladed propeller operating with and without a downstream wing based on the Dornier 217 geometry. Using the Sliding Mesh approach in ANSYS Fluent, unsteady simulations were conducted to capture the transient effects of rotating flow fields. The domain was divided into a rotating region for the propeller and a stationary zone for the wing to replicate realistic conditions. Results show that the inclusion of the wing within the propeller slipstream alters flow behavior—leading to increased local velocity and static pressure near the wing, along with a slight reduction in thrust output compared to the standalone propeller case. These trends align with prior literature and underline the importance of careful aerodynamic integration in propeller-driven aircraft systems.

Keywords: Propeller, Dornier 217, ANSYS Fluent, CFD

I. INTRODUCTION

The integration of propellers with fixed-wing aircraft presents a complex aerodynamic challenge, especially in configurations where the propeller operates upstream of the wing. This arrangement is widely observed in small-scale unmanned aerial vehicles (UAVs), regional commuter aircraft, and emerging electric vertical takeoff and landing (eVTOL) platforms. In such systems, the interaction between the rotating propeller and the stationary aerodynamic surfaces introduces intricate flow dynamics. These include variations in local velocity fields, pressure distributions, and vortex structures, which in turn influence the lift, drag, and thrust characteristics of the overall system. Properly accounting for these effects is critical to ensuring aerodynamic efficiency, structural safety, and energy optimization in integrated propulsion designs.

Conventional aerodynamic analysis of propeller-wing systems has often relied on experimental wind tunnel tests or simplified analytical models. While these methods provide foundational understanding, they frequently fall short in capturing the transient nature of propeller-induced flow fields. Recent advancements in computational fluid dynamics (CFD), however, offer the capability to resolve unsteady interactions with high accuracy. Among these, the Sliding Mesh technique has emerged as a robust tool to model rotating machinery by allowing the mesh around the rotating domain to move independently of the stationary surroundings. This is particularly important in analysing propeller wake development, slipstream contraction, and pressure gradients that arise due to the proximity of aerodynamic surfaces like wings or fuselages.

In this study, a numerical investigation is carried out to evaluate the aerodynamic influence of a downstream wing placed in the slipstream of a tractor-type propeller. The wing used in the simulation is modeled after the Dornier 217 aircraft, chosen for its conventional straight-wing geometry. Simulations are performed in two configurations: a standalone propeller and a propeller with a wing located immediately downstream. The goal is to compare the thrust output, velocity field, and static pressure distribution in both cases using transient CFD simulations in ANSYS Fluent. The insights gained from this analysis contribute toward a better understanding of how such interactions affect propulsion performance and can aid in future aerodynamic optimization of integrated aircraft systems. The aerodynamic interaction between propellers and wings has emerged as a critical design consideration in both conventional and modern aircraft configurations, particularly in low-speed UAVs, distributed propulsion systems, and electric vertical takeoff and landing (eVTOL) platforms. These interactions can significantly affect lift augmentation, thrust efficiency, and overall aerodynamic stability. Recent research has shown that slipstream-induced flow changes around downstream surfaces are

IARJSET ISSN (O) 2393-8021, ISSN (P) 2394-1588

International Advanced Research Journal in Science, Engineering and Technology

Impact Factor 8.066 ⁑ Peer-reviewed & Refereed journal ⁑ Vol. 12, Issue 4, April 2025

DOI: 10.17148/IARJSET.2025.124104

complex and require high-fidelity modeling to understand accurately. Experimental and numerical studies such as those by Della Vecchia et al. [6], Srivathsan et al. [7], and NASA Langley Research Center [11] have emphasized the importance of resolving unsteady effects when analyzing propeller-wing systems. Additionally, advancements in CFD have enabled detailed investigation of propeller-induced wake characteristics and pressure fields [8][10].

II. METHODOLOGY

A. Geometry Modelling

The design was created in SolidWorks, where the 3D models of the three-bladed propeller and the Dornier 217 wing were developed., modelled as a three-bladed configuration. The design corresponds to a scaled-down version of a full-scale propeller with a diameter of 3.0 meters. The scaled model features a radius of 280 mm, resulting in a geometric scaling factor (λ) of 10.714. This factor was applied to adjust both the rotational speed and thrust values according to aerodynamic similarity principles. The aircraft wing integrated in the study is based on the Dornier 217 planform, selected for its historical aerodynamic relevance and its moderate aspect ratio, which makes it suitable for propeller-wing interaction analysis.

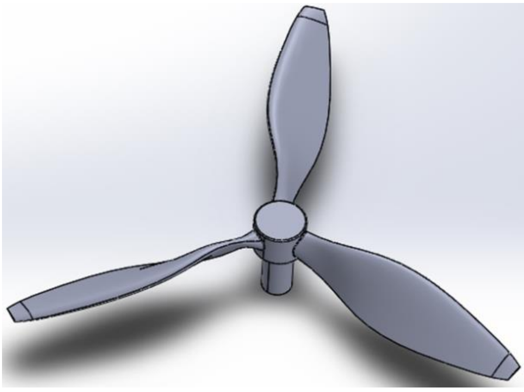

Fig.1: Designed Propeller

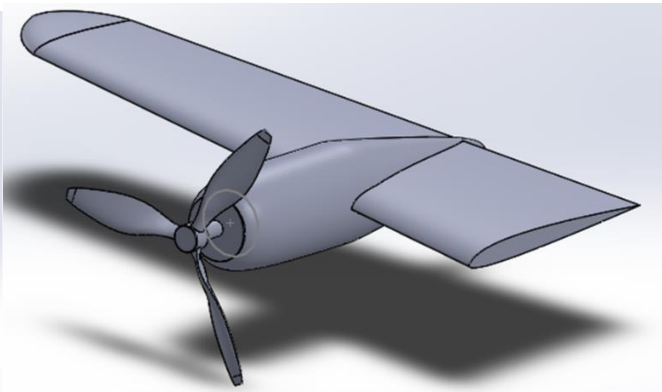

Fig.2: Isometric View of the Propeller Wing Integration

Figure 1 illustrates a three-bladed propeller designed in SolidWorks using the MH-112 airfoil profile, known for its high aerodynamic efficiency at low Reynolds numbers. The model features evenly spaced blades with a smooth twist and taper distribution, optimized for thrust generation in small-scale propulsion systems.

Figure 2 presents the integrated model of a three-bladed propeller mounted on a Dornier aircraft wing, which was designed and assembled using SolidWorks. The configuration demonstrates the propeller-wing interaction setup, where the MH112-based propeller is positioned at the wing's leading edge to analyses aerodynamic coupling effects
The flow domain was split into a rotating cylindrical zone surrounding the propeller and a larger stationary enclosure accommodating the wing and free stream. Boolean operations were used to subtract overlapping volumes between these zones.

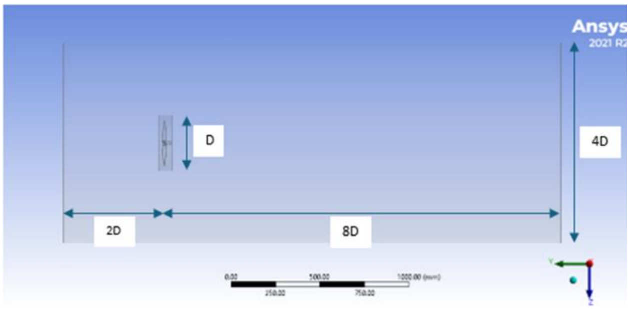

Fig.3: Stationary & Rotating Domains

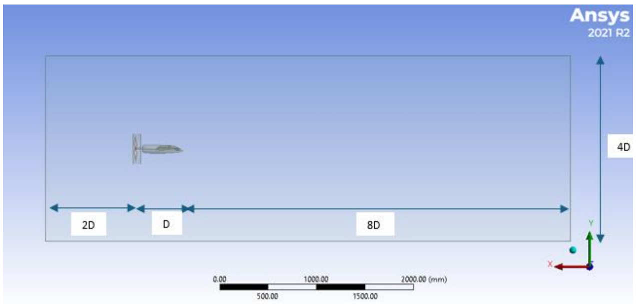

Fig.4: Propeller &Wing in The Stationary Fluid Domain

The Figure 3 shows the stationary and rotating domains dimensions where D = 280 mm. Rotating domain diameter is 280 mm and the Stationary domain diameter is 4D (1120 mm), whereas Figure 4 demonstrates the stationary and rotating domains of the propeller wing integration where D = 470 mm.

IARJSET ISSN (O) 2393-8021, ISSN (P) 2394-1588

International Advanced Research Journal in Science, Engineering and Technology

Impact Factor 8.066 ⋇ Peer-reviewed & Refereed journal ⋇ Vol. 12, Issue 4, April 2025

DOI: 10.17148/IARJSET.2025.124104

Rotating domain diameter is 280 mm and the Stationary domain is a rectangular domain of dimensions Length = 11 D, Breadth = 2.5 D and Height = 4 D (5170mm × 1175mm × 1880mm).

B. Meshing

A high-resolution, unstructured mesh was generated to accurately capture the flow field around the rotating propeller and its downstream interaction with the wing. The meshing process was carried out in ANSYS Workbench using tetrahedral elements, with refined controls applied based on geometric sensitivity and anticipated flow gradients.

For the propeller-only configuration, a structured preprocessing approach was adopted. A cylindrical rotating domain was created around the propeller, encapsulated within a larger stationary domain representing the freestream. The rotating zone was discretized with a fine element size of 2 mm, ensuring adequate resolution of blade curvature, tip vortices, and near-field wake behavior. The outer stationary domain was assigned an element size of 8 mm, sufficient to resolve free-stream conditions and capture downstream flow structures. Inflation layers comprising eight layers with a growth rate of 1.2 were applied to all solid boundaries to resolve boundary layers and improve near-wall accuracy. The mesh contained approximately 4.9 million nodes and 29 million elements, and skewness and orthogonality metrics were maintained within acceptable limits (skewness < 0.25, orthogonal quality > 0.8).

For the propeller–wing integrated case, the domain was extended to accommodate the wing inside the slipstream. The domain dimensions were increased to 5170 mm × 1175 mm × 1880 mm to allow for complete development of the wake and downstream pressure recovery.

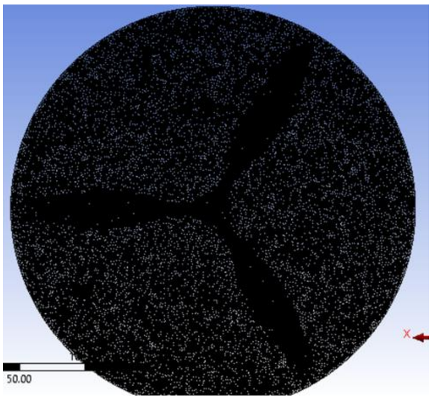

Fig.5: Meshing of the Propeller

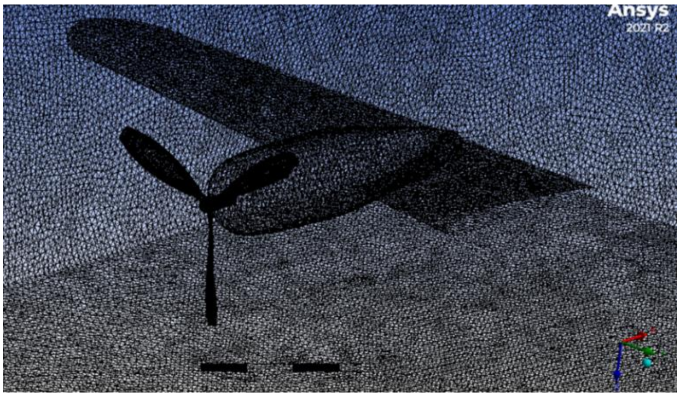

Fig.6: Meshing of the Propeller-Wing Integration

Figure 5 is the illustration of mesh generated using ANSYS Fluent. A refined mesh is applied near the blades to accurately resolve the flow field and aerodynamic behaviour.

Figure 6 shows the mesh generated in ANSYS Fluent for the propeller–wing integrated model; similar meshing strategies were applied but with additional face sizing controls on the wing surface and edge sizing on leading and trailing edges to capture detailed pressure distributions and local acceleration zones. The mesh count increased to approximately 9.3 million nodes and 54.6 million elements in this configuration, the mesh is refined near the propeller and wing surfaces to capture detailed flow interactions and ensure accurate aerodynamic analysis.

C. Fluent Setup and Calculation

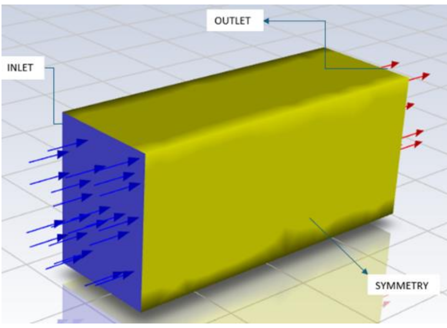

Fig.7: Boundary conditions of the setup

IARJSET

ISSN (O) 2393-8021, ISSN (P) 2394-1588

International Advanced Research Journal in Science, Engineering and Technology

Impact Factor 8.066 ⁙ Peer-reviewed & Refereed journal ⁙ Vol. 12, Issue 4, April 2025

DOI: 10.17148/IARJSET.2025.124104

Figure 7 illustrates the boundary conditions defined for propeller-wing configuration in ANSYS Fluent. The setup includes a velocity inlet to specify the incoming airflow, a pressure outlet to allow flow exit, and wall boundaries applied to the propeller, wing, and surrounding domain surfaces. The rotating region around the propeller is defined using a sliding mesh or rotating reference frame, enabling realistic simulation of the propeller's motion and its interaction with the wing's flow field.

Simulations were conducted in ANSYS Fluent using a pressure-based coupled solver with a transient formulation to resolve the unsteady flow around the rotating propeller. The realizable k–ω turbulence model was chosen for its ability to handle rotating flows and near-wall effects effectively. The Sliding Mesh approach was applied between the rotating and stationary domains to capture the physical motion of the propeller blades. A velocity inlet was defined with a freestream velocity of 130 m/s, and a pressure outlet with a gauge pressure of 0 Pa was used downstream. All solid surfaces were set as no-slip walls. Time steps were selected to correspond to 1° of propeller rotation per step, ensuring temporal resolution of blade-passing events, and the simulation was run for several revolutions until periodic convergence in thrust was achieved. Rotational speeds were varied from 100 to 1400 RPM in increments, and thrust, velocity, and pressure fields were extracted for each case to assess performance trends.

III. RESULT AND DISCUSSION

Simulations were carried out for rotational speeds ranging from 100 RPM to 1400 RPM, in order to investigate the aerodynamic behaviour of both the standalone propeller and the propeller–wing integrated configuration. For each case, key performance indicators such as thrust, exit velocity, and static pressure were extracted and compared. Although results were recorded at multiple operating conditions, the outcomes for 600 RPM are presented in detail as a representative case, while overall trends across all RPMs are analysed in the subsequent sections.

A. Performance at 600 RPM

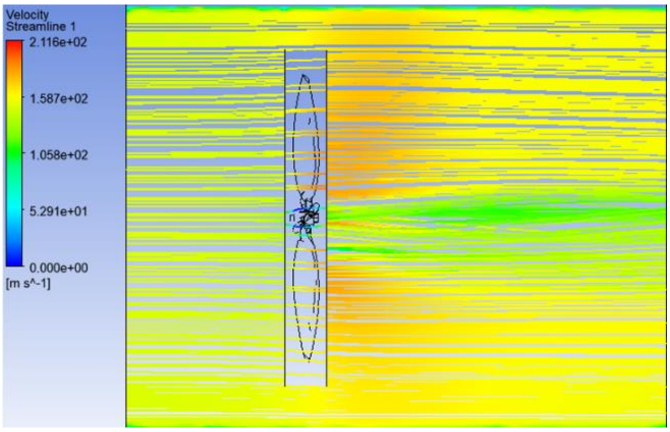

Fig.8: Velocity Streamline of the Propeller Stand alone at 600 RPM

Figure 8 shows Velocity streamlines around the standalone propeller operating at 600 RPM. The flow pattern shows the rotational effects and induced velocity field created by the spinning blades, highlighting areas of acceleration and wake development behind the propeller.

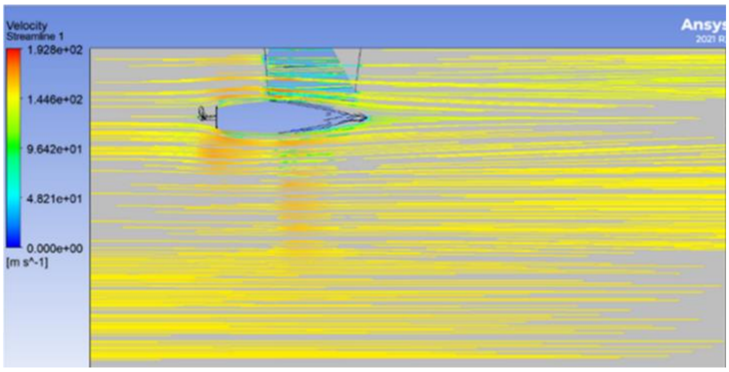

Fig.9: Velocity Streamline of the Propeller-Wing Integration at 600 RPM

IARJSET ISSN (O) 2393-8021, ISSN (P) 2394-1588

International Advanced Research Journal in Science, Engineering and Technology

Impact Factor 8.066 ⁖ Peer-reviewed & Refereed journal ⁖ Vol. 12, Issue 4, April 2025

DOI: 10.17148/IARJSET.2025.124104

Figure 9 illustrates velocity streamlines for the integrated propeller-wing configuration at 600 RPM. The propeller's wake interacting with the wing surface is clearly visible indicating changes in flow behaviour due to the combined aerodynamic effects .

At 600 RPM, contour plots of velocity and static pressure were extracted for both configurations. In the propeller-only case, a well-formed slipstream was observed with uniform acceleration along the axial direction. The thrust generated was higher compared to the integrated case due to the unobstructed development of the wake. In the propeller-wing configuration, the wing introduced aerodynamic interference, altering the slipstream structure and resulting in localized increases in velocity and static pressure near the wing surface. However, this came at the cost of a slight reduction in overall thrust, attributed to flow disruption and wake interaction. These results are consistent with published literature, where the insertion of lifting surfaces within a propeller's slipstream often leads to wake distortion and thrust loss.

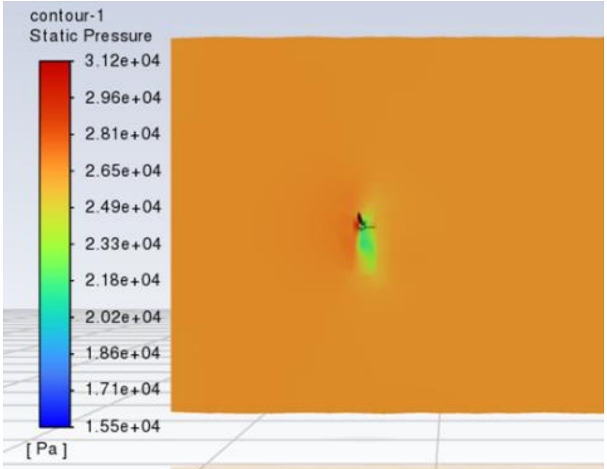

Fig 10 Static Pressure of the Propeller -Wing Integration at 600 RPM

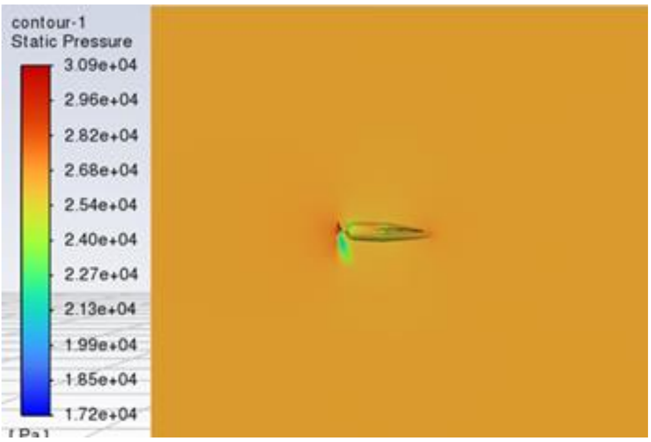

Fig. 11: Static Pressure of the Propeller Stand alone at 600 PM

Figure 10: Static Pressure of the Propeller–Wing Integration at 600 RPM The pressure variation along the blade surfaces illustrates the thrust-generating regions and the suction effect on the upstream side of the blades.

Figure 11 shows static pressure distribution for the standalone propeller at 600 RPM. Compared to the integrated setup, the standalone configuration at 600 RPM shows more uniform pressure gradients. indicating greater thrust and more intense aerodynamic loading on the blades.

DOI: 10.17148/IARJSET.2025.124104

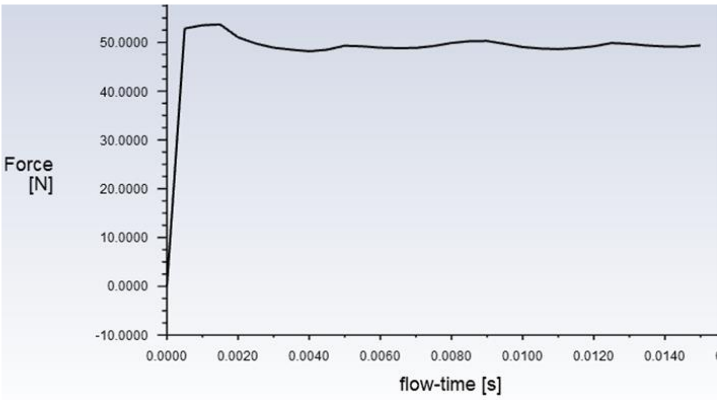

Fig.12: Thrust plot of the Propeller at 600 RPM

Figure 12 illustrates the thrust plot produced by the integrated system at this rotational speed, highlighting the aerodynamic interactions between the propeller and the wing.

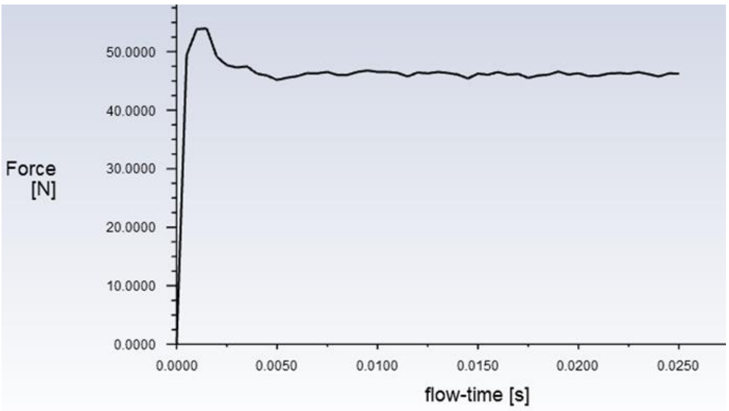

Fig.13: Thrust plot of the Propeller-Wing Integration at 600 RPM

Figure 13 shows thrust plot for the Propeller-Wing Integration at 600 RPM. Due to the presence of wing in the downstream the thrust has been decreased than compared to propeller stand alone case.

B. RPM vs Thrust

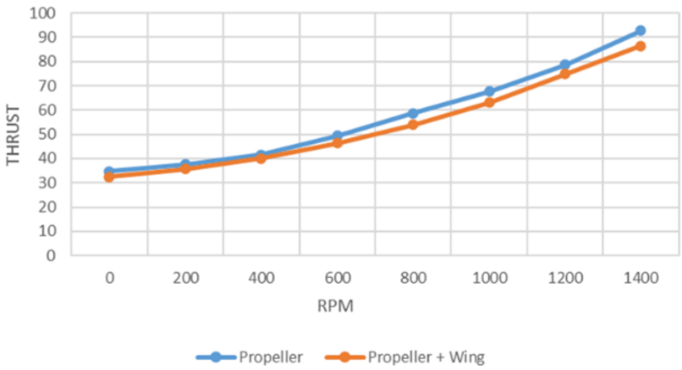

Fig.14: RPM vs Thrust

Figure 14 shows the plot of RPM versus thrust generation. As RPM increases, thrust also increases. This subsection presents the variation of thrust with RPM for both configurations. A clear upward trend is observed in both cases; however, the propeller-only configuration consistently produced higher thrust across all RPMs. The thrust difference becomes more pronounced at higher RPMs due to increased wake momentum and greater interference in the integrated case.

IARJSET ISSN (O) 2393-8021, ISSN (P) 2394-1588

International Advanced Research Journal in Science, Engineering and Technology

Impact Factor 8.066 ⁜ Peer-reviewed & Refereed journal ⁜ Vol. 12, Issue 4, April 2025

DOI: 10.17148/IARJSET.2025.124104

C. RPM vs Velocity

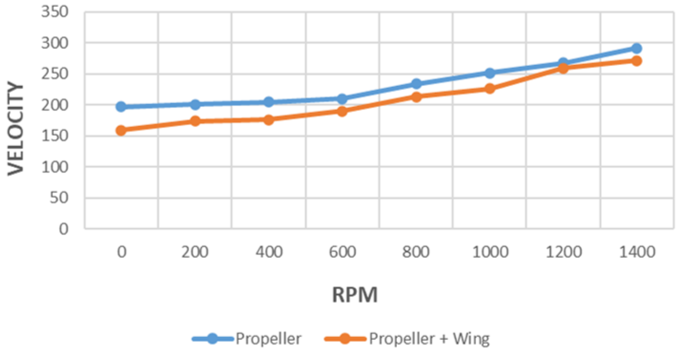

Fig.15: RPM vs Velocity

Figure 15 presents the graph showing the variation of velocity with RPM for two configurations: a propeller alone and a propeller combined with a wing. As RPM increases from 0 to 1400, both configurations exhibit a clear upward trend in velocity, indicating that higher rotational speeds result in greater airflow velocity.

The flow velocity extracted from the slipstream centreline shows a steady increase with RPM for both configurations. However, peak velocities in the propeller-only case are consistently higher, due to the absence of downstream obstruction. The presence of the wing in the integrated setup induces pressure gradients that decelerate and redistribute the wake.

D. RPM vs Static Pressure

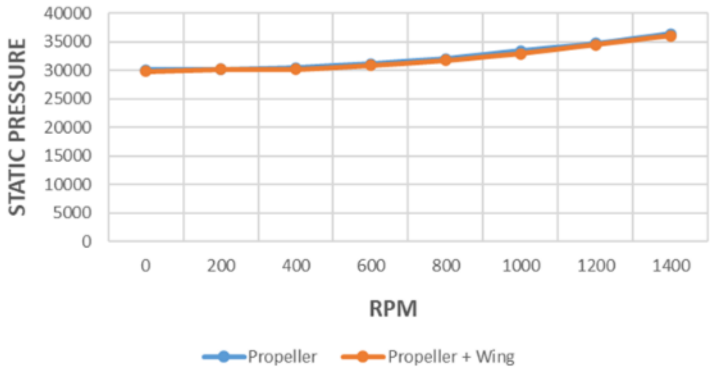

Fig.16: RPM vs Static Pressure

The graph illustrates the relationship between static pressure and rotational speed (RPM) for two configurations: a standalone propeller and a propeller combined with a wing. Across the entire range of RPMs (0 to 1400), both configurations show a positive correlation between RPM and static pressure, indicating that as the propeller spins faster, the static pressure increases.

Static pressure was measured at downstream monitoring planes. While pressure increased with RPM in both setups, the propeller-only configuration exhibited greater pressure recovery. The wing in the integrated case caused localized pressure buildup near its leading edge but reduced overall static pressure in the wake due to energy dissipation and flow separation effects.

IV. CONCLUSION

This numerical study has provided a comprehensive analysis of the aerodynamic interactions between a rotating propeller and a downstream wing, focusing on a scaled Dornier 217 configuration. By simulating both standalone and integrated setups across various rotational speeds using the Sliding Mesh method in ANSYS Fluent, the investigation revealed critical insights into how slipstream effects influence thrust generation and flow behaviour.

The results consistently demonstrated that the presence of a wing downstream of the propeller causes a modest but measurable reduction in thrust—typically in the range of 5–8%—due to wake interference and altered pressure gradients.

DOI: 10.17148/IARJSET.2025.124104

Despite this reduction, the integrated configuration exhibited localized increases in velocity and static pressure near the wing's leading edge, highlighting the complex trade-offs involved in propeller-wing coupling. These findings are in strong agreement with existing literature, validating the simulation approach and the scaling methodology adopted. The use of high-fidelity meshing, accurate turbulence modelling, and realistic operating conditions has ensured that the outcomes are both reliable and relevant for practical aircraft design.

Future work could include optimization of axial separation, blade twist, and wing incidence angles to further enhance performance and mitigate interference effects

E. VALIDATION

The numerical simulations in this study showed that the standalone propeller configuration outperformed the integrated propeller-wing setup in terms of thrust, exit velocity, and static pressure. This reduction in performance in the integrated configuration is mainly due to flow interference between the propeller slipstream and the wing, which causes distortion, pressure buildup, and deceleration of the flow. Several studies support these findings, including McCormick (1995) and Bertin (1998), who discuss how the wing's position within the slipstream reduces thrust and efficiency [1]. Additional research from Liang et al. (2009) and Sinnige et al. (2008) [confirms that positioning the wing within the slipstream leads to performance losses [2],[3]. Furthermore, Oliveira & Hallak (2019) noted that isolated propellers generate more uniform flow, while integrated systems require careful optimization to recover performance [10]. Anderson (2006) also highlighted that integrating lifting and propulsive surfaces can affect boundary layer behaviour and momentum recovery, potentially reducing aerodynamic output [4],[5]. These findings are consistent with both experimental and numerical research.

REFERENCES

[1]. B. W. McCormick, Aerodynamics, Aeronautics, and Flight Mechanics, John Wiley & Sons, 1995.
[2]. T. Sinnige, G. Nitzsche, and R. Veldhuis, "Modeling Propeller-Wing Interactions Using Vortex-Lattice Methods," AIAA Journal, vol. 56, no. 5, pp. 1892–1904, 2018.
[3]. Y. Liang, R. Haritos, and X. Zhang, "URANS Simulation of eVTOL Wing-Propeller Configuration," Journal of Aircraft, vol. 59, no. 2, pp. 445–457, 2022.
[4]. J. D. Anderson, Introduction to Flight, 8th ed., McGraw-Hill, 2016.
[5]. J. D. Anderson, Fundamentals of Aerodynamics, 6th ed., McGraw-Hill, 2011.
[6]. Pierluigi Della Vecchia, G. Maddalena, and G. Quaranta, "Experimental and Numerical Study of Propeller-Wing Configurations," STAR-CCM+ Applications in Aerospace, 2015.
[7]. Srivathsan et al., "Interactional Aerodynamics of Propeller-Wing Systems," AIAA Aviation Forum, 2020.
[8]. J. Wang, M. Liang, and H. Wang, "Propulsive Wing Concepts for eVTOL Applications," Aerospace Science and Technology, vol. 124, pp. 107–119, 2023.
[9]. S. Ahmad et al., "Performance Metrics and Optimization of Propeller-Wing Integration," Energies, vol. 11, no. 10, pp. 2831–2844, 2018.
[10]. R. A., N. L., & P. H. Hallak, "Aerodynamic Analysis of Propellers by Computational Fluid Dynamics," Proceedings of the Conference, pp. 1-8, 2019, Federal University of Juiz de Fora.
[11]. NASA Langley Research Center, "Effects of Slipstream on Lift and Thrust," Technical Memorandum, NASA-TM-2003-211234, 2003.